# THE CRYSTAL STRUCTURE OF BERTHIERITE, $FeSb_2S_4$

M. J. Buerger and Theodor Hahn, *Crystallographic Laboratory, Department of Geology and Geophysics, Massachusetts Institute of Technology, Cambridge, Massachusetts.*

Abstract

The general arrangement of atoms in berthierite had been suggested in an earlier publication by solving the Patterson function $P(xy)$, with the aid of the minimum function $M_8(xy)$. In this paper a report is given of the refinement of the structure. The intensities were measured by the M.I.T. modification of the Dawton method, and the resulting $F^2$'s were placed on an absolute basis by Wilson's method. The structure was refined by the use of successive difference Fourier syntheses. The final structure has a small residual factor and neatly reproduces the Patterson projection.

In the structure of berthierite each Sb atom is evidently bonded to 3 S atoms at distances of about 2.5 Å. These $SbS_3$ groups share S atoms to form two non-equivalent $SbS_2$ chains parallel to the $c$ axis. The Fe atoms are surrounded by 6 S atoms in approximately octahedral arrangement at distances of about 2.5 Å. This is about the expected distance for ionic Fe-S bonds. The structure can therefore probably be regarded as $Fe^{++}(SbS_2)_2^-$.

## Introduction

*Material.* The berthierite from Kisbánya, Carpathians, has been described in detail by Zsivny and Zombory (1934). These investigators were kind enough to make a generous sample of this material available for this crystal-structure investigation. The analysis of the Kisbánya berthierite indicates that it has almost exactly the ideal composition $FeSb_2S_4$.

*Unit cell and space group.* The unit cell and space group of berthierite have been reported in an earlier communication (Buerger, 1936). The cell has the following dimensions:

$$a = 11.44 \text{ Å}$$
$$b = 14.12$$
$$c = 3.76$$

This cell contains $4FeSb_2S_4$. The space group is *Pnam*.

*Intensity determination.* The structure determination reported here was based upon *hk*0 and *h*0*l* reflections as recorded on precession photographs. The intensities were determined by using the M.I.T. modification of the Dawton (1938) method. The intensities were corrected for Lorentz and polarization factors, but no allowance was made for absorption.

In the course of the structure determination it became evident that the $F$ values determined in this manner were accurate and quite satisfactory except that there is a critical lower intensity below which one cannot distinguish a non-zero intensity from zero intensity. The lack of knowledge of the $F$'s having amplitudes between zero and the lowest observable amplitude was keenly felt as the refinement progressed.

TABLE 1. COORDINATES OF ATOMS FOR DIFFERENT TRIALS

| | | Trial | | | | | | | | | | |
|---|---|---|---|---|---|---|---|---|---|---|---|---|
| | | 1 | 2 | 3 | 4 | 5 | 6 | 7 | 8 | 9 | 10 | 11 |
| $Sb_I$ | $x$ | .147 | .148 | .149 | .149 | .149 | .148 | .145 | .140 | .143 | .145 | .145 |
| | $y$ | .060 | .059 | .059 | .063 | .063 | .063 | .064 | .063 | .063 | .062 | .062 |
| $Sb_{II}$ | $x$ | .040 | .044 | .041 | .037 | .037 | .038 | .036 | .041 | .039 | .037 | .037 |
| | $y$ | .384 | .382 | .381 | .387 | .387 | .386 | .385 | .386 | .386 | .386 | .386 |
| Fe | $x$ | .321 | .318 | .318 | .323 | .323 | .321 | .314 | .320 | .316 | .316 | .317 |
| | $y$ | .340 | .336 | .337 | .339 | .339 | .337 | .335 | .335 | .334 | .334 | .335 |
| $S_I$ | $x$ | .190 | .204 | .200 | .230 | .200 | .200 | .197 | .197 | .196 | .195 | .194 |
| | $y$ | .270 | .273 | .273 | .290 | .273 | .270 | .272 | .272 | .272 | .272 | .272 |
| $S_{II}$ | $x$ | .414 | .419 | .421 | .417 | .421 | .424 | .428 | .428 | .426 | .424 | .423 |
| | $y$ | .200 | .186 | .187 | .198 | .187 | .185 | .186 | .186 | .185 | .184 | .185 |
| $S_{III}$ | $x$ | .240 | .229 | .230 | .237 | .230 | .227 | .229 | .229 | .227 | .226 | .226 |
| | $y$ | .485 | .495 | .494 | .484 | .494 | .493 | .494 | .494 | .492 | .492 | .492 |
| $S_{IV}$ | $x$ | .452 | .452 | .450 | .418 | .450 | .451 | .452 | .452 | .450 | .451 | .451 |
| | $y$ | .408 | .407 | .407 | .388 | .407 | .404 | .405 | .405 | .406 | .405 | .405 |

TABLE 2. $R$ FACTORS FOR $F_{hk0}$ FOR DIFFERENT TRIALS

| | | 3 | 4 | 5 | 6 | 7 | 8 | 9 | 10 | 11 |
|---|---|---|---|---|---|---|---|---|---|---|
| R, % | (*a*) | 19.0 | 27.3 | 17.1 | 14.7 | 15.8<br>14.2* | 14.3* | 12.4* | 12.8* | 13.2* |
| | (*b*) | 17.8 | 26.4 | 16.0 | 12.6 | 13.2<br>12.3* | 12.2* | 10.2* | 10.8* | 11.1* |
| | (*c*) | 24.5 | 38.5 | 22.5 | 19.1 | 19.8<br>18.6* | 19.3* | 16.8* | 17.1* | 17.3* |
| | (*d*) | 23.3 | 37.4 | 19.8 | 17.2 | 17.6<br>16.8* | 17.2* | 14.7* | 15.1* | 15.3* |

(*a*) $\Delta F = F_o - F_c$ omitted if $F_o = 0$.
(*b*) $\Delta F = F_o - F_c$ omitted if $\Delta \leqq$ least significant difference.
(*c*) When $F_o = 0$, it is assigned a mean value between true zero and least observable $F_o$.
(*d*) Condition *b* and *c* together.
* New scale.

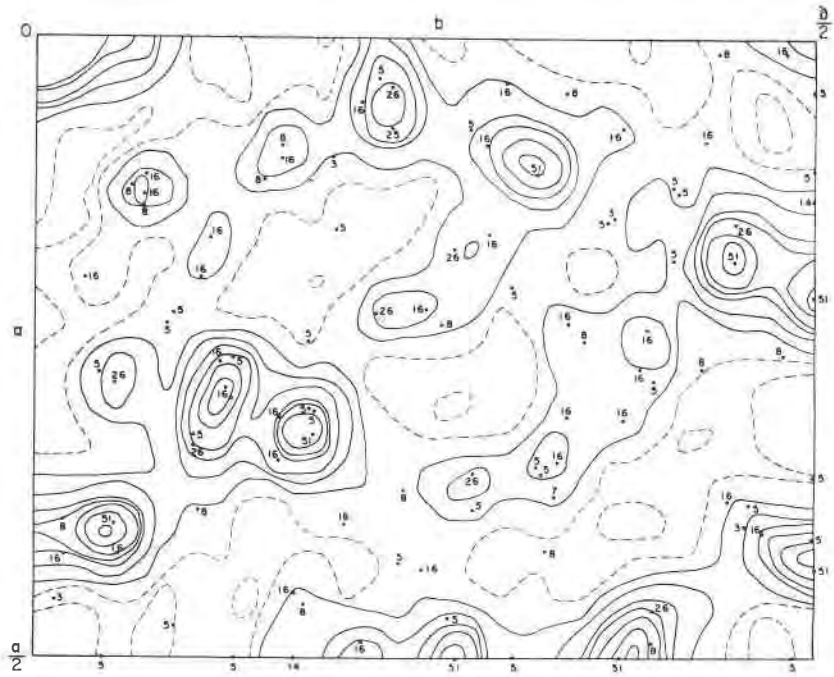


FIG. 1. Patterson projection of berthierite, $P(xy)$. Dots and accompanying numbers show weighted vector set for the final structure.

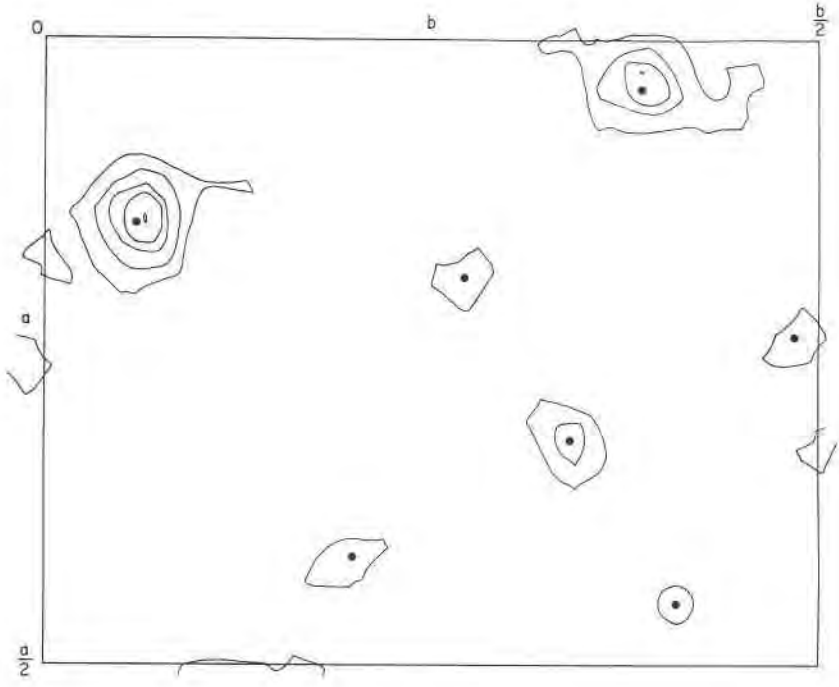


FIG. 2. The minimum function, $M_8$. Dots show the positions of the atoms as derived from the minimum function.

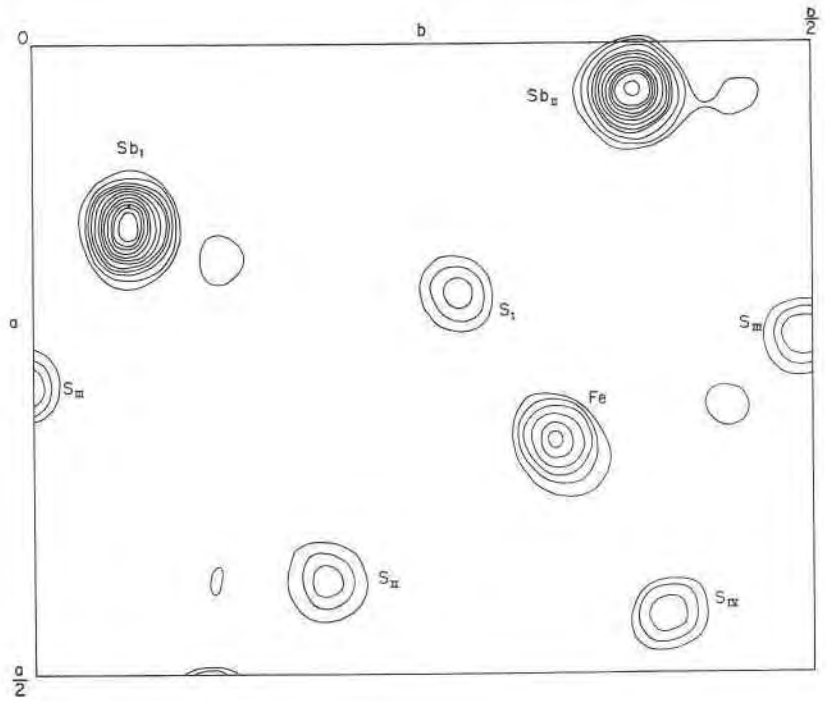


FIG. 3. The electron density map, $\rho(xy)$ of berthierite.

## APPROXIMATE LOCATIONS OF ATOMS

Rough intensity considerations had already shown that all atoms of berthierite were confined to the (001) reflection planes, that is, to equipoint 4*c*, for which $z = \pm\frac{1}{4}$. With the aid of the $F^2_{hk0}$'s, a Patterson projection $P(xy)$ was prepared, Fig. 1. In another place (Buerger, 1951) it was shown that this projection could be solved for the $xy$ coordinates of the atoms by applying the minimum function (Buerger, 1950). The approximate electron density found by this method is shown in Fig. 2. The several dense areas, in order of decreasing density, are evidently the two antimony atoms, the one iron atom, and the four sulfur atoms. The close relation of this minimum function map to the true structure can be appreciated by comparing it with Fig. 3, the electron density projection $\rho(xy)$, as determined after refinement.

There is an interesting peculiarity about an approximate structure determined by image-seeking methods: one must make a decision regarding the location of at least the first image point. The location of the one atom corresponding to this image point is fixed by this choice and

does not change in the course of applying the image-seeking function to find the other atoms of the structure. There is usually a small error involved in selecting an image point. For example, an error arises when the Patterson peak chosen for the image point is not a single peak, but rather the coalescence of several peaks not in exactly the same location. At this stage of the analysis one cannot usually determine to what extent the peak is composite. This image-point error remains as a slight error in the location of the corresponding atom. The error can only be removed by a subsequent refinement process.

## Preliminary Refinement

The structure of berthierite as found by image-seeking methods was believed to be essentially correct with regard to the general location of the atoms, since there was a rough agreement between computed and observed intensities. Nevertheless this agreement was not good. Refinement of this structure was evidently necessary. It was carried out in

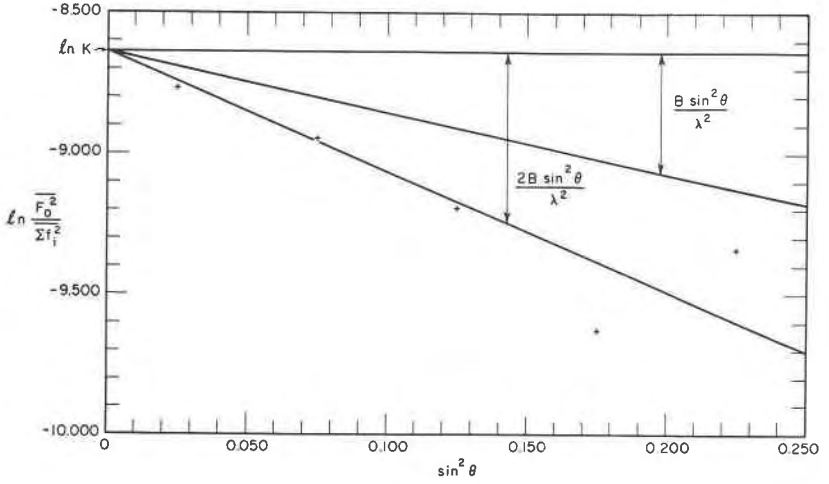


Fig. 4. Determination of absolute scale and temperature factor for $F_{hk0}$ by Wilson's method.

eleven stages. The migration of coordinates during the refinement is outlined in Table 1.

For the purpose of refining the structure, the observed $hk0$ intensities were placed on an absolute basis using Wilson's (1942) method, Fig. 4. This analysis not only places the intensities on an absolute basis but also yields the temperature coefficient $B$. The value of this turned out to be 1.07 Å$^2$ for berthierite. The value of $B$ and the absolute scale of intensi-

ties were slightly improved when the structure was considerably refined.

The original structure as determined with the aid of the minimum function was termed *trial 1*. This was examined to ascertain what obvious shifts in atom locations would improve agreement between calculated and observed intensities. This predicted an improved set of atom locations which was called *trial 2*. This procedure was repeated, resulting in an improved set of atom locations called *trial 3*.

## Further Refinement

*Residual factor*. This marked the end of elementary methods of refining the structure. From this stage onward, the status of the refinement was followed by computing the observed and computed amplitude residual factor (Robertson and Woodward, 1936)

$$R = \frac{\Sigma\big|\,|F_{\text{observed}}| - |F_{\text{calculated}}|\,\big|}{\sum |F_{\text{observed}}|}. \qquad (1)$$

The magnitude of this factor varies somewhat depending upon how one treats the smallest $F_o$ and the smallest differences, $\Delta = F_o - F_c$. In Table 2 we have computed four types of $R$, labelled $(a)$, $(b)$, $(c)$, and $(d)$. These are defined in Table 2.

*Refinement by Patterson maps*. The first non-elementary refinement procedure made use of comparing the weighted vector set of trial 3 with the observed Patterson map. These showed reasonably good agreement, but

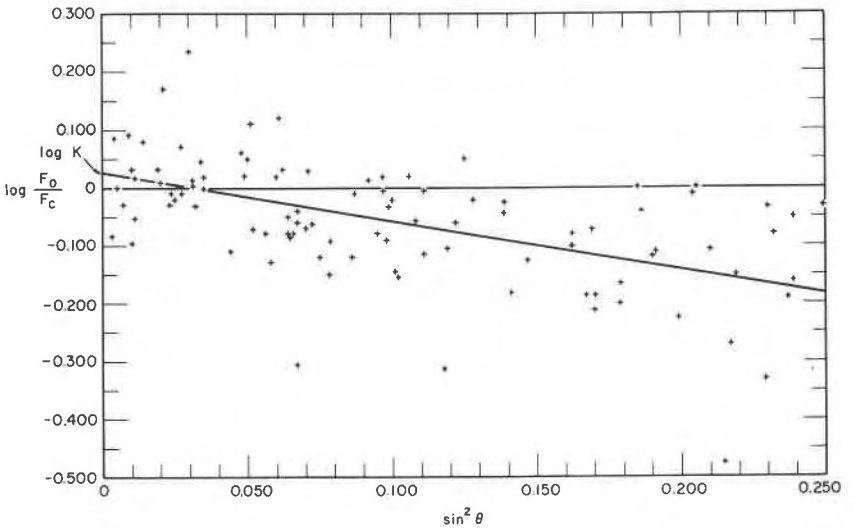


Fig. 5. Final refinement of absolute scale of $F_{hk0}$ of berthierite.

detailed comparison indicated that the agreement could be improved by some small shifts in the locations of some atoms. This improved structure was termed *trial 5*. Another set of atom locations, called *trial 4*, differs from trial 5 only in that the sulfur atoms had been moved to idealized covalent octahedral locations about iron. Table 1 shows that the residual factor for the ideal sulfur arrangement was so much worse that the possibility of an idealized $FeS_6$ group was evidently excluded.

From this point on the structure was refined chiefly by difference syntheses (Cochran, 1951), using as Fourier coefficients $(F_{\text{observed}} - F_{\text{computed}})_{hk0}$. This synthesis is known to minimize $R$.

*First difference synthesis.* The set of amplitudes $F_c$, computed from trial 5 (resulting from the refinement-by-Patterson procedure) was used to compute a difference synthesis, Fig. 6. The atom locations proved to be on gradients on this map, so the locations were shifted up-gradient to produce a new set of locations, namely *trial 6*. The change from trial 5 to trial 6 reduced the residual factor from 17.1% to 14.7%.

*Electron density projection, $\rho(xy)$.* At this point it was believed that the structure was in a sufficient state of refinement to warrant preparing an electron density projection, $\rho(xy)$. This shown in Fig. 3. The peak locations of $\rho(xy)$ are taken as *trial 7*. Although the coordinates of trial 6 and trial 7 are different, they do not correspond to any changes in phase of $F_{hk0}$. Thus Fig. 3 may be taken as the final electron density map. The weighted vector set of trial 7 is shown superposed on the corresponding Patterson map in Fig. 1. The agreement between them is quite good, so that the structure may be said to neatly explain the Patterson synthesis.

In spite of the fact that Fig. 3 is the final $\rho(xy)$, the locations of its peaks do not provide the best values of the coordinates. This is obvious on studying Table 1. Trial 7 has a larger $R$ value than trial 6. Furthermore, starting with trial 7, whose coordinates are derived from $\rho(xy)$, it is possible to obtain other sets of coordinates by refinement which have smaller $R$ values, and without changing the phases of any $F_{hk0}$'s. That a set of $F_{hk}0$'s produces a map, $\rho(xy)$, whose peaks deviate slightly from the exact atom locations is due to using a finite set of $F_{hk0}$'s in the synthesis. This is the series-termination effect. This effect is substantially absent in differential syntheses. The residual termination effect does not change the general course of the lines of the difference map, and consequently the gradient is insensitive to slight errors in the $F$'s. On the other hand a peak maximum in $\rho(xz)$ is, in general, shifted by the termination effect. The study given here presents detailed evidence that difference syntheses are superior to electron-density syntheses for refinement.

*New scale factor.* Up to this point the scale factor derived by Wilson's method had been used. Since no further sign changes were in prospect,

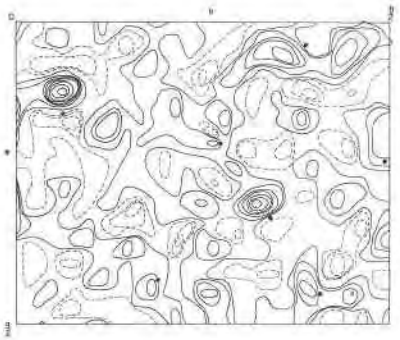

FIG. 6

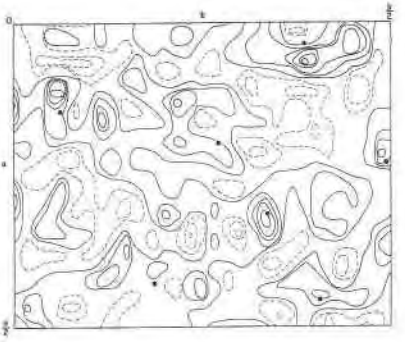

FIG. 7

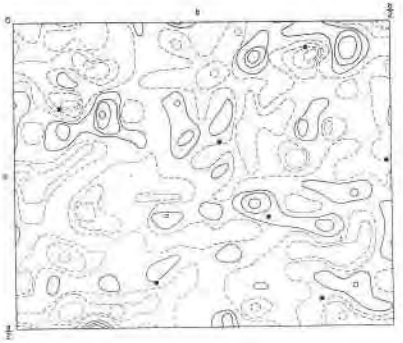

FIG. 8

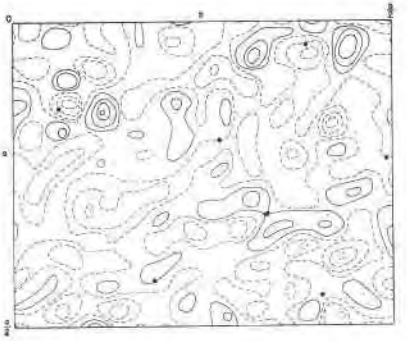

FIG. 9

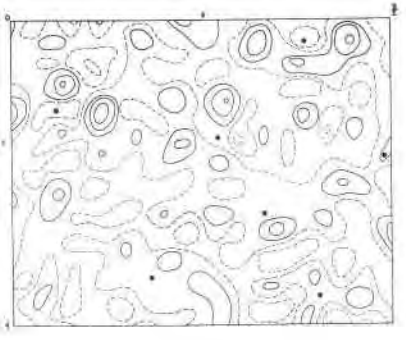

FIG. 10

FIGS. 6, 7, 8, 9, 10. Difference maps, $\rho_o - \rho_c$, for successive trial structures. The positions of atoms used for the $\rho_c$ part of the particular difference map are shown by dots.

the structure was regarded as sufficiently well-settled to permit computing a new refined scale factor, by plotting $\log |F_o| / |F_c|$ against $\sin^2\theta$. This is shown in Fig. 5. The change in the scale factor in going from

Wilson's method to this method proved to be from 75.5 to 71.0, while $B$ changed from 1.07 $A^2$ to 0.98 $A^2$. The use of the new scale factor reduced the $R$ factor from 15.8% to 14.2%.

*Further refinement by difference synthesis.* Trial 7 was further refined by a series of difference syntheses shown in Figs. 7, 8, 9, and 10. In these figures the atom locations used for the difference syntheses are shown as black dots. The criterion for correct atom position is that the original atom locations are found to lie on positions of zero gradient on the difference map. In each trial, therefore, the dots were moved up-gradient in the hope that the subsequent synthesis would show them to lie on zero gradient.

In order to find the parameter range within which the Sb's must lie, these were moved by .005 from trial 7 to *trial* 8. This move proved to be too much, as indicated by the sharp reversal of gradient which accompanied the shift. Subsequent trials have Sb parameters between the values used for trial 7 and trial 8.

The Fe and three of the S atoms assumed positions of substantially zero gradient by *trial 9*. In *trial 10* the other atoms are also in zero-gradient position but the Fe atom again appears to lie on a slight gradient. This is probably due to contributions from other atoms and therefore signifies that refinement of the Fe position has been achieved within the accuracy of our data. *Trial 11* was devised to give the Fe and 2 S's a slight shift to improve their positions on gradients. This last set of shifts produced a set of parameters having higher $R$ values. Trial 10 was accordingly accepted as the final set of parameters since the atoms are all on substantially zero gradient even though its $R$ value is slightly greater than that of trial 9.

After computing this set of difference syntheses, it became evident that a shift of parameters of .001 or .002 changes the configuration of the map strongly and in such a way as to reverse the gradient, at least for the heavier atoms when they are in the neighborhood of the correct locations. From this it is deduced that the accuracy of the final atomic coordinates given for berthierite is about .002, which is equivalent to about .02 Å. It is of interest to note that when the atoms are in the neighborhood of their final correct positions the major features of the difference map coincide with the background of the electron density map. The features of the difference map must, therefore, be regarded as due chiefly to errors in the determination of the $F_o$'s.

## Selection of $z$ Parameters

The $xy$ coordinates of all atoms in the structure are now known with accuracy. Since the atoms are confined to the reflection planes, their co-

TABLE 3. $R$ FACTORS FOR $F_{h0l}$

| | |
|---|---|
| (*a*) | 8.8% |
| (*b*) | 5.9% |
| (*c*) | 8.8% |
| (*d*) | 5.9% |

(See Table 2 for explanation of conditions *a*, *b*, *c*, and *d*.)

ordinates can be either $\frac{1}{4}$ or $-\frac{1}{4}$. The only combination which was acceptable was found by making a limited number of intensity computations for $F_{h0l}$. A complete set of $F_{h0l}$'s was computed based upon this combination. These were independently placed on an absolute basis by comparing observed and computed intensities. The resulting temperature factor, $B$, for the $h0l$ reflections proved to be 0.99, compared with 0.98 found previously for the $hk0$ reflections. The resulting $R$ values are shown in Table 3. The electron-density projection $\rho(xz)$ is shown in Fig. 11. In this projection some of the atoms are unresolved due to overlapping.

## THE FINAL STRUCTURE

The electron density projections for the entire cell are shown in proper relation in Fig. 12. The final parameters are given in Table 4. A comparison of observed and computed $F$ values is filed with the American Documentary Institute.*

## DISCUSSION OF THE STRUCTURE

The distances between neighboring atoms in berthierite are listed in Table 5. These distances are shown in a diagrammatic representation of the structure in Fig. 13.

It is convenient to discuss the structure of berthierite in two stages. In the first stage account is taken only of the nearest neighbors. Table 5 and Fig. 13 show that each of the two kinds of Sb atoms has three

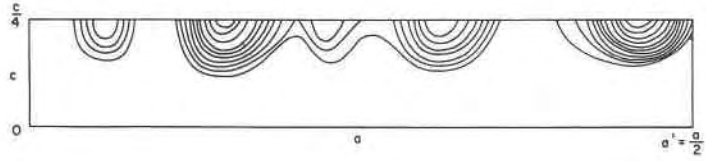


FIG. 11. The electron density map $\rho(xz)$ of berthierite.

* A copy may be secured by writing to the ADI Auxiliary Publications Project, Photoduplication Service, Library of Congress, Washington 25, D. C., and requesting Document number 4189. Advance payment of $1.25 is required for photoprints, or $1.25 for 35 mm. microfilm. Make checks payable to: Chief, Photoduplication Service, Library of Congress.

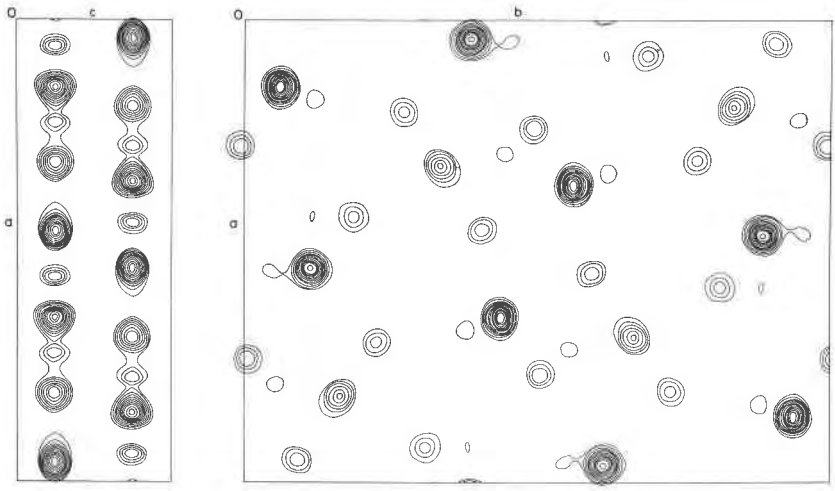


FIG. 12. Relation between the electron density projections $\rho(xy)$ (right), and $\rho(xz)$ (left), for the full cell of berthierite.

nearest S neighbors at distances of about 2.5 Å, as well as other S atoms at larger distances. The Sb and S atoms thus form $SbS_3$ groups. Each group shares two of its three S atoms with translation-equivalent groups to form $SbS_2$ chains parallel to the $c$ axis.

The Fe atoms are surrounded by six S atoms in approximately octahedral arrangement. These octahedra share edges to form chains parallel to the $c$ axis. The Fe-S distance is about 2.5 Å. This is considerably in excess of that found in structures where the bonds are recognized as covalent (pyrite, 2.26 Å, marcasite, 2.24 Å). The distance is about what would be expected for ionic Fe-S bonds. Thus, the structure of berthierite suggests that its chemical nature is $Fe^{++}(SbS_2)_2^{-}$. Curiously enough, the $Sb_I$ triangles share an edge with each of two neighboring Fe octahedra, whereas the $Sb_{II}$ triangles only share corners with these octahedra.

TABLE 4. FINAL COORDINATES OF ATOMS IN BERTHIERITE

| | $x$ | $y$ | $z$ |
|---|---|---|---|
| $Sb_I$ | 0.145 | 0.062 | $+\frac{1}{4}$ |
| $Sb_{II}$ | 0.037 | 0.386 | $-\frac{1}{4}$ |
| Fe | 0.316 | 0.334 | $+\frac{1}{4}$ |
| $S_I$ | 0.195 | 0.272 | $-\frac{1}{4}$ |
| $S_{II}$ | 0.424 | 0.184 | $+\frac{1}{4}$ |
| $S_{III}$ | 0.226 | 0.492 | $+\frac{1}{4}$ |
| $S_{IV}$ | 0.451 | 0.405 | $-\frac{1}{4}$ |

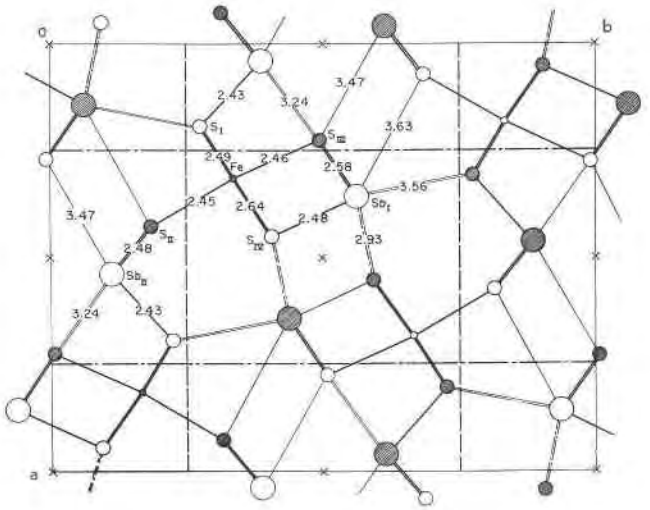


FIG. 13. Interatomic distances in berthierite. Shaded circles represent atoms on level $+\frac{1}{4}$, while open circles represent atoms on level $-\frac{1}{4}$.

Each of the four kinds of sulfur atoms in berthierite is coordinated to three metal atoms and each such set of metals contains both Fe and Sb atoms.

If one takes account of second small inter-atomic distances then it becomes evident that the two kinds of Sb atoms are quite different. The $Sb_{II}$ has no further neighbors nearer than 3.2 Å while $Sb_I$ has two additional neighbors at about 2.9 Å. This rather small distance doubtless represents a bond, so that one can also describe the $Sb_I$ atoms as forming irregular $SbS_5$ groups. Two such $SbS_5$ groups, related by the inversion center in the middle of Fig. 13, share the two second-nearest S's with

TABLE 5. INTERATOMIC DISTANCES IN BERTHIERITE

| | $S_I$ | $S_{II}$ | $S_{III}$ | $S_{IV}$ |
|---|---|---|---|---|
| $Sb_I$ | 3.56 (2) | 3.63 (1) | 2.58 (2) | 2.48 (1)<br>2.93 (2) |
| $Sb_{II}$ | 2.43 (1) | 2.48 (2) | 3.24 (2)<br>3.47 (1) | |
| Fe | 2.49 (2) | 2.45 (1) | 2.46 (1) | 2.64 (2) |
| $S_I$ | 3.76 (2) | 3.45 (2) | 3.64 (2) | |
| $S_{II}$ | | 3.76 (2) | | 3.66 (2) |
| $S_{III}$ | | | 3.76 (2) | 3.43 (2) |
| $S_{IV}$ | | | | 3.76 (2) |

Note: Numbers in parentheses indicate the number of distinct vectors of this length.

each other so that a complex chain of composition $Sb_2S_4$ can be discerned parallel to the $c$ axis. An alternative description is that the two $SbS_2$ chains, related by the inversion center in the middle of Fig. 13, can be regarded as joined so as to form more complex chains of composition $Sb_2S_4$. This kind of double chain has also been discovered in livingstonite (Buerger and Niizeki, 1954). The two kinds of sulfur coordination displayed by $Sb_{II}$ and $Sb_I$ atoms are also found in the two types of Sb atoms of stibnite.

The Fe atom appears to have the function of cementing together the two kinds of $SbS_2$ chains. It should be noted that the coordination of Fe is irregular octahedral. Four of the S atoms are at distances of about 2.46 Å but two more are at distances of 2.64 Å. This condition is quite real since an attempt to regularize the distances resulted in a much higher $R$ value.

The cleavage of berthierite is reported in one reference as more or less distinct parallel to one pinacoid, and in another reference as rather distinct prismatic. Fig. 13 shows that a cleavage could occur parallel to (010) without the breaking of any bonds except the 2.93 Å bond from $Sb_I$ to $S_{IV}$.

ACKNOWLEDGMENT

This research was supported by the Office of Naval Research under Contract No. *N5ori-07860* with the Massachusetts Institute of Technology.

REFERENCES

BUERGER, M. J. (1936), Crystallographic data, unit cell and space group for berthierite ($FeSb_2S_4$): *Am. Mineral.*, **21,** 442–448.

BUERGER, M. J. (1950), Limitation of electron density by the Patterson function: *Proc. Nat. Acad. Sci.*, **36,** 738–742.

BUERGER, M. J. (1951), A new approach to crystal-structure analysis: *Acta Cryst.*, **4,** 531–544.

BUERGER, M. J., AND NIIZEKI, NOBUKAZU (1954), The crystal structure of livingstonite, $HgSb_4S_7$; *Am. Mineral.*, **39,** 319–320.

COCHRAN, W. (1951), The structures of pyrimidines and purines. V. The electron distribution in adenine hydrochloride: *Acta Cryst.*, **4,** 81–92.

DAWTON, RALPH H. V. M. (1938), The integration of large numbers of $x$-ray reflections: *Proc. Phys. Soc.*, **50,** 919–925.

ROBERTSON, J. MONTEATH, AND WOODWARD, IDA (1936), The structure of the carboxyl group. A quantitative investigation of oxalic acid dihydrate by Fourier synthesis from the $x$-ray crystal data: *J. Chem. Soc. Lond.*, 1817–1824, esp. p. 1822.

WILSON, A. J. C. (1942), Determination of absolute from relative $x$-ray intensity data: *Nature,* **150,** 151–152.

ZSIVNY, VICTOR, AND ZOMBORY, LÁSZLÓ (1934), Berthierite from Kisbánya, Carpathians: *Mineral. Mag.*, **23,** 566–568.

*Manuscript received Jan. 20, 1954.*